Pak. J. Bot., 51(4): 1263-1271, 2019. DOI: http://dx.doi.org/10.30848/PJB2019-4(18)

DNA BARCODING AND PHYLOGENY OF *PHLOMIS AUREA* (LAMIACEAE) ENDEMIC TO SINAI PENINSULA, EGYPT

AHMED EL-BANHAWY[1*] AND WIDAD AL-JUHANI[2]

[1]*Botany Department, Faculty of Science, Suez Canal University, Ismailia, Egypt, PO. Box 41522*
[2]*Biology Department, Faculty of Applied Science, Umm Al-Qura University, Makkah, Saudi Arabia,*
[*]*Corresponding author's email: ahmedbanhawy@hotmail.com*

Abstract

Taxonomy represents the baseline for biological characterization and naming for endangered plant species. *Phlomis aurea* has never been a subject of comprehensive biosystematics assessment. *Phlomis aurea* is an endangered species suffering from global changes which lead to population decline. It is important to rediscover critical biological traits related to endemic species to help set up conservation plan(s). The current study represents a comprehensive morphological and anatomical characterization of the endangered *Phlomis aurea* endemic to Sinai Peninsula, Egypt. Phylogenetic placement and DNA barcoding were done using two molecular markers (*rbc*L and *psb*-A/*trn*-H).

Key words: DNA barcoding, endemic, *Phlomis aurea*, phylogeny, Sinai, *psb*-A/*trn*-H, *rbc*L.

Introduction

The genus *Phlomis* L., belongs to the family Lamiaceae and subfamily Lamioideae. It comprises more than 100 species, mainly concentrated in the Mediterranean basin. It is native to Turkey, North Africa, Europe and Asia.

According to Khafagi *et al.,* (2013), of the approximately 900 plant species in the Sinai Peninsula, 28 of these are endemic. One-third of the endemic plant species in South Sinai, including *Phlomis aurea*, have been recorded in the Saint Katherine area (Fig. 1).

The flowering parts of *Phlomis* are generally used as an herbal tea for its taste and aroma as well as to treat gastrointestinal troubles and to promote good health by protecting the liver, kidney, bones and cardiovascular system. Moreover, the pharmacological activities of some *Phlomis* species have been proven to be anti-diabetic, anti-nociceptive, anti-ulcerogenic, anti-inflammatory, anti-allergic, anticancer, antimicrobial and antioxidant; they also protect the vascular system (Leticia *et al.,* 1980).

Taxonomic studies based on morphological, anatomical and pollen grain characteristics have been carried out to differentiate between closely related *Phlomis* species (Firdous *et al.,* 2015). Bentham (1832) used the corolla shape as a diagnostic trait to divide the genus *Phlomis* L. into two groups: *Phlomoides* and *Phlomis*. The latter was further subdivided into three sub-groups: *Dendrophlomis*, *Gymnophlomis* and *Oxyphlomis*. Yetişen (2014) showed that the most important distinctive features for *Phlomis monocephala* were the presence of raphide crystals in the leaf, the phloem fibres and the structure of the trichomes. Oran (2015) differentiated six species of *Phlomis* from Jordan based on pollen grain morphology. Cali (2016) studied *Phlomis russeliana*, endemic to Turkey, investigated various anatomical characteristics such as the number of pith rays in the root, the number of palisade and spongy parenchyma layers in the leaf, the types of stomata and the petiole anatomy.

Despite these studies, identification based on macro- and micro-morphological traits might be difficult and misleading when differentiating between closely related species. Many plant genera have been re-identified using molecular techniques such as Random Amplification of Polymorphic DNA (RAPD) (Yuzbasioglu *et al.,* 2008), microsatellite (Karaca *et al.,* 2013) and DNA barcoding (Theodoridis *et al.,* 2012, Faried1 *et al.,* 2018).

The main objective of this study is to provide a comprehensive characterization of the medicinally important endemic *Phlomis aurea* in Egypt using macro- and micro-morphological traits, DNA barcoding and phylogenetic analysis.

Materials and Methods

Sampling: The current study is based on both herbarium and freshly collected specimens from their natural habitats in the Wadi El-Arbaeen sub-basin area, Saint Katherine protectorate, South Sinai, Egypt. All locations were accurately recorded using a Whistler Galileo GPS-100 Handheld GPS Receiver, USA (Figs. 1 and 2).

Each specimen collected from the field was vouchered by 3–5 specimens. All studied specimens were deposited in the herbarium of Suez Canal University (SCUI).

Portions of fresh leaf materials were kept in plastic pages containing silica gel for molecular experiments. Another lot of leaf parts and stems were kept in 70% ethanol until transferred to the laboratory of the Biology Department, Faculty of Applied Science, Umm Al-Qura University, Makkah, Saudi Arabia, for the anatomical experiments. The anatomical analyses of the stems and leaves were carried out according to the conventional method of Johansen (1940). Examination of the specimens was carried out and photos were taken with a Balplan microscope (Bausch & Lomb, USA). Measurements were taken using ImageJ 1.46r software, USA after calibration, using a standard image.

Taxonomic characterization: Both the fresh and herbarium materials were examined carefully. To describe the macro and micro morphological feature, glycerine jelly mounting medium slides were prepared using 10 gm of gelatine dissolved into 60 ml distilled water that was stirred continuously over gentle heat (65°C) until dissolution was complete, and then 70 ml of glycerine was added. For preservation of the medium, 1 ml of phenol was added. For nomenclature including the synonyms Boulos (2002), Feinbrun-Dothan (1986) and Täckholm (1974) were followed.

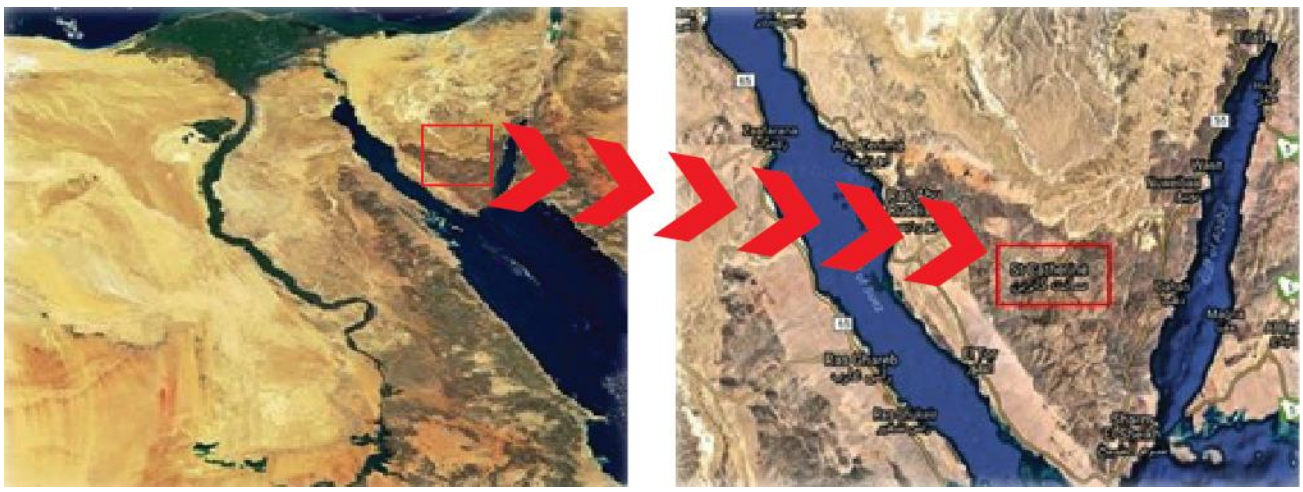

Fig. 1. Map of sampling area (Sinai Peninsula, Egypt).

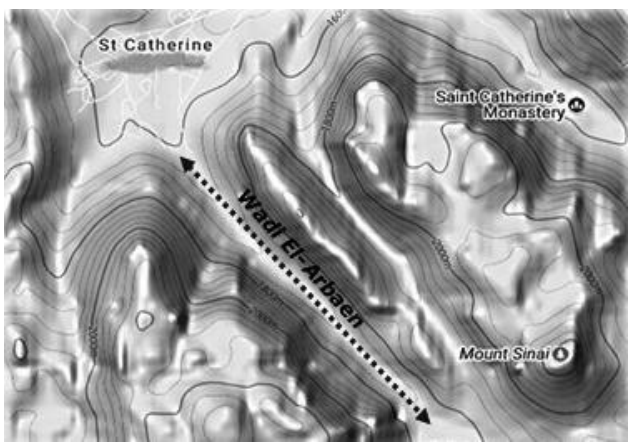

Fig. 2. Wadi El-Arbaeen sub-basin area.

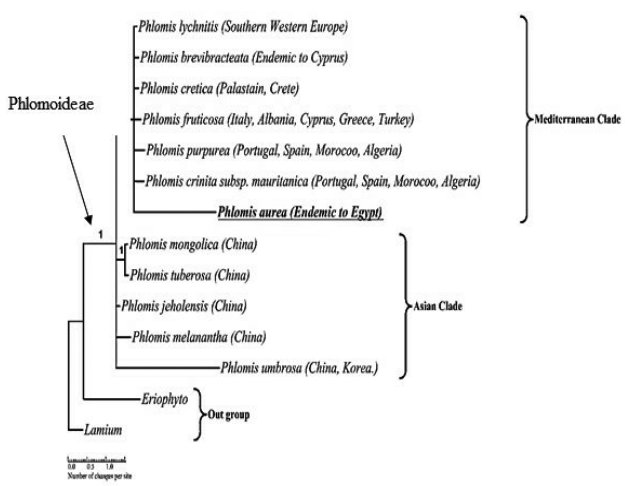

Fig. 3. Bayesian all-compatible phylogenetic tree inferred from concatenated datasets of two cpDNA markers (*psb*-A/*trn*-H and *rbc*L) of *Phlomis aurea*; Number above branches = posterior probability (PP).

Molecular characterization

DNA extraction: Total genomic DNA was isolated from 0.01–0.1 g of herbarium or silica gel-dried leaves, using hot hexadecyltrimethylammonium bromide (CTAB) after Doyle & Doyle (1987), which was modified by adding 2% polyvinyl pyrrolidone (PVP) 40 to the buffer (2% CTAB, 20 mM EDTA, 1.4 mM NaCl and 100 mM Tris-HCl, pH 8) to improve the quality of the DNA.

Polymerase chain reaction (PCR): Double-stranded DNA was amplified with a PCR using previously published primer sets: *psb*-A/*trn*-H (Sang *et al.,* 1995) and *rbc*L (Kress *et al.,* 2009; Levin *et al.,* 2003). The thermal cycler Veriti™ Dx 96-well, 0.2 ml (Applied Biosystems®, USA) was used. The reaction was carried out according to the manufacturer's instructions in 25 µl BioMix® (Bioline, UK), a complete, ready-to-use 2x reaction mix containing an ultra-stable DNA polymerase for bidirectional sequencing. To enhance amplification, bovine serum albumin (BSA) was added to the PCR aliquot prior to the start of the reaction. The PCR was carried out using the following protocol: BioMix™ = 12.5 µl, 10 µM forward primer (Sigma-Aldrich) = 1 µl, 10 µM forward primer (Sigma-Aldrich) = 1 µl, 10 mg/3 ml BSA = 1 µl, DD water = 8.5 µl, DNA template = 1~2 µl, total reaction volume = 25 µl.

The chloroplast DNA (cpDNA) markers *psb*-A/*trn*-H as well as *rbc*L have been used as barcodes and to reconstruct the phylogeny of *Phlomis aurea* species. The following PCR protocol was used for the intergenic spacer *psb*-A/*trn*-H: 94°C for 2 min; 30 cycles of 94°C for 2 s; 53°C for 1 min; 1 min at 72°C; final extension at 72°C for 7 min. The *rbc*L PCR protocol was as follows: 98°C for 45 s; 35 cycles of 98°C for 10 s; 55°C for 30 s; 72°C for 40 s; final extension at 72°C for 10 min.

PCR purification and DNA sequencing: PCR products were purified using a QIA quick PCR purification kit, QIAGEN, Germany. For DNA sequencing, a second PCR was performed using a BigDye Terminator v3.1 Cycle Sequencing Kit, USA for a total volume of 20 µl; each reaction contained 8 µl terminator-ready reaction mix, 3.2 pmol primer, a DNA template (template quantity was calculated according to the PCR product size), and deionized water.

The thermal profile for the cycle sequencing PCR was as follows: 96°C for 1 min, 25 cycles at 96°C for 10 s, 72°C for 5 s; final extension at 60°C for 4 min. After an additional purification step using Centri-Sep columns (Princeton Separations, USA), DNA sequencing was applied with the 3500 genetic analyser (Applied Biosystem, USA).

Bioinformatics

Data preparation: Novel sequences of *psb*-A/*trn*-H and *rbc*L markers were generated for the available specimens. GenBank services were used to: (1) validate the new sequences against previously published data using the Basic Local Alignment Search Tool (BLAST) and (2) download the available sequences needed to construct balanced data sets for the operational taxonomic unit (OUT) for both DNA barcoding and phylogenetic analysis.

Sequence alignment: FASTA-formatted files containing the sequences were exported to BioEdit version 7.0 (Hall 1999) for alignment. The DNA sequences were aligned in multiple alignments using the ClustalW 1.83 software package with the default settings (Thompson *et al.,* 1994). Gaps were treated as missing data. Alignment curation was carried out using the Gblocks algorithm that was available under the advanced analysis option on http://www.phylogeny.fr/ (Dereeper *et al.,* 2010).

Phylogenetic analysis: Bayesian phylogenetic inferences (BI) were conducted using MrBayes software (ver. 3.2) (Ronquist *et al.,* 2012). Three independent datasets were analysed. These were made up of two types: single locus datasets (two datasets) and a concatenated dataset of both cpDNA markers. The optimal nucleotide substitution model (GTR + I + G) was selected for each alignment via Akaike information criterion (AIC) (Akaike, 1974) using PAUP (Swofford, 2003) and the MrModelblock command from MrModeltest (Nylander, 2004).

For each matrix, two independent Bayesian analyses were performed to check for convergence with four chains per analysis, and the trees were sampled every specified number of generations relevant to each dataset. All datasets were run for one million generations.

All compatible trees were calculated in MrBayes. A plot of negative log likelihoods against generation time was calculated using the Markov chain Monte Carlo (MCMC Tracer Analysis) tool (ver. 1.6.0, 2003) to establish the burn-in (Rambaut *et al.,* 2013). Trees found before reaching stability were pruned out, and the rest were used to compile an all-compatible tree. The all-compatible tree was exported to TreeGraph 2 (ver. 2.0.50-314 beta) software for visualization and editing (Stöver & Müller, 2010). Posterior probabilities (PP) were used to measure clade support.

DNA barcoding: BLAST offers a trusted tool to anticipate the probability of DNA sequences of selected markers such as *psb*-A/*trn*-H and *rbc*L to use as barcodes. For correct identification, the BLAST percent identity for the query sequence should be the highest among the expected species belonging to the expected genera. The identification is considered ambiguous when the BLAST percent identity matches several genera of the expected family. Incorrect identification means that the BLAST percent identity for a query sequence retrieved species/genera not belonging to the expected species/genera (Chase *et al.,* 2007).

Results

Sample collection: Five populations of *Phlomes aurea* from Wadi El-Arbaeen were selected. The exact locations of the collected specimens were as follows: 28° 33′ 27.4032″ N 33° 56′ 3.9696″ E, 28° 33′ 58.8816″ N 33° 54′ 45.7416″ E, 28° 34′ 1.326″ N 33° 54′ 58.7196″ E, 28° 34′ 1.0524″ N 33° 54′ 55.6308″ E and 28° 33′ 14.1012″ N 28° 33′ 14.1012″ N. The elevation of the study area ranged from 1580 to 1660 m. A variety of landforms was recorded, including the wadi bed, slopes and terraces (Figs. 1 and 2).

Morphological characterization

***Phlomis aurea* Decne. (*Ann. Sci. Nat., Bot., sér 2, 2:251 [1834]*); (Figs. 4-5):**

Perennial herbs or sturdy vigorous shrubs, often woolly or felty, 50–150 cm high. Leaves simple, entire, estipulate, opposite, decussate, cuneate at base, wrinkled or corrugated, with crenate margins and densely covered with whitish or mostly yellowish stellate hairs; lower cauline leaves oblong to oblong-ovate (8–15 mm long x 8–16 mm wide), with obtuse tips; upper cauline leaves broadly lanceolate (25–50 mm long x 10–17 mm wide). Petiole of the upper leaves 5–15 mm long; of lower leaves 4–16 mm long. Floral leaves lanceolate, 15–20 mm long x 3–5 mm wide. Verticillasters three to five clusters with 10 flowers each, the distance between the clusters is 5–10 cm; bracteoles few (not more than two) for each verticil; 10–15 mm long x 3–5 mm wide, floral leaves as long as the verticillasters or longer. Calyx tubular-campanulate, 14–19 mm long, distinctly folded, 10-ribbed, striate, hairy, divided into five unequal lobes; the three anterior lobes longer and narrower than the two posterior lobes, truncate with minute straight prickles instead of teeth; the prickles equalling the anterior lobes (1–3 mm long), and the posterior lobes with shorter prickles (0.5–1 mm long). Corolla bi-labiate, yellow (including the tube), mostly hairy, ringed inside below the middle of the tube and as long as the calyx or slightly longer; the upper lip densely hairy and helmet-shaped; the lower lip spreading with lateral lobes, 20–30 mm wide. Stamens four, ascending under the upper lip, epipetalous and didynamous, the anterior stamens longer; the filaments of the posterior stamens appendiculate at the base, anther 2-celled, dorsifixed and dehiscing longitudinally. One gynobasic style arising from the central depression of the ovary lobes. Stigma bifid, the branches subulate and unequal; the posterior branch shorter than the anterior one. Pollen grain ovoid, tricolpate and papillose.

Fruit with 4 nutlets enclosed within a persistent calyx. Seed ovoid-triquetrous, obtuse, with an acute apex, slightly hairy.

Table 1. Indumentum and trichome types of *Phlomis aurea*.

		Non-glandular				Glandular				
		Simple unbranched	Stellate			(Capitate)			Dendroid	
			sub-type I	sub-type II	sub-type III	sub-type I	sub-type II	sub-type III	sub-type I	sub-type II
Leaf	Upper epidermis	+	+	+	-	+	+	+	-	-
	Lower epidermis	+	-	-	+	-	-	-	-	+
Bract		-	-	-	-	-	+	-	+	-
Stem		-	+	-	-	+	+	+	+	-
Calyx		+	-	-	-	-	-	-	+	-
Corolla		+	-	-	-	-	-	-	+	-

Capitate trichome: sub-type I = (basal cell: 1; stalk: 1; head: 2); **sub-type II** = (basal cell: 1; stalk: 2–3; head: 1); **sub-type III** = (basal cell: 1; stalk: 1; head: 4). **Stellate trichome: sub-type I** = (basal cell buried into epidermis and three branches); **sub-type II** = (multicellular base carried on raised epidermis with three branches); **sub-type II** = (four-celled stalk that ends with four branches); **Dendroid trichome: sub-type I** = **(**branches 4–10); **sub-type II** = (branches: 7–9)

Table 2. Micro-morphological measurements in µm of leaf and stem

Anatomical traits	Petiole		Leaf		Stem	
	Ave.	SE	Ave.	SE	Ave.	SE
Epidermis (proximal)	19	0.23	34.75	0.53	23.93	0.25
Epidermis (adaxial)	-	-	-	0.14	-	
Parenchyma	86.70	0.219	-	-	84.66	0.32
Collenchyma	34.65	0.119	-	-	14.22	0.41
Cambium	11.88	0.119	38.90	0.23	48.34	0.54
Phloem	36.46	0.375	97.71	0.36	41.13	0.78
Xylem	67.73	0.151	132.77	0.52	83.61	0.48
Palisade layer	-	-	106.52	0.41	-	-
Spongy layer	-	-	177.41	0.46	-	-
Pith	-	-	-	-	647.00	0.90

Ave. = Average measurement, SE = Standard deviation

Indumentum (**Fig. 6)**

The indumentum of the leaf, petiole, bract, stem, calyx and corolla were found to be useful taxonomic characteristics at a specific level. The indumentum of *Phlomis aurea* was highly variable (Table 1). The indumentum consisted of three main types of trichomes: (1) non-glandular trichomes, simple or stellate (2) glandular capitate trichomes and (3) dendroid trichomes. The non-glandular trichomes are represented by simple, unbranched, bi-cellular uni-seriate trichomes that are present on the leaves, calyx and corolla. Moreover, non-glandular, multi-cellular, bi-seriate trichomes are present on the lower epidermis of the leaves. Three sub-types of non-glandular stellate trichomes were recorded. The first sub-type consists of one basal cell buried into the epidermis and the two branches; this sub-type was present on the upper epidermis of the leaf and stem. The second sub-type was present on the upper epidermis of the leaf and consists of a multi-cellular base carried on a raised epidermis with three branches. The third type of stellate trichome was present on the lower epidermis of the leaf, and it consisted of a four-celled stalk that ended into four branches. Three sub-types of glandular capitate trichomes were recorded. Sub-type I was composed of a basal cell bearing a short uni-cellular stalk and bi-cellular head; it was found on the leaf, petiole and stem. Sub-type II comprised of a basal cell bearing two to three stalks and a mono-cellular head; this type was recorded on the bract, leaf, petiole and stem. Sub-type III is composed of a basal cell bearing a mono-cellular stalk; it ended with a four-celled head found on the leaf, petiole and stem. Dendroid trichomes were recorded on the stem and lower epidermis of the leaf. It consists of a tree-like structure with 4-10 branches on the stem (sub-type I) and 7-9 on the leaf (sub-type II).

Stem anatomy (Fig. 7 & Table 2)

Stem is quadrangular in a cross section and consists of three layers: cortex, a ring of vascular bundles and thick pith. Cuticle is relatively thick. Epidermis is radially and tangentially elongated, with one to two layers of barrel-shaped parenchyma cells. Three kinds of trichomes were recorded: stellate, glandular capitate and dendroid trichomes (see indumentum section and Table 1). Cortex has one to two layers of lacunar collenchyma, followed by 4-7 layers of oval-shaped parenchyma cells, with four angular collenchyma patches determined at the corners; the cortex layer ends with a wavy, starchy sheath consisting of a single row of parenchyma cells filled with starch grains. Pericycle consisted of 2-4 layers of sclerenchyma cells concentrated around and enclosing the central vascular cylinder, forming a wide discontinuous ring. A continuous ring of pen vascular bundles and sclerenchyma fibres produced by the interfascicular cambium gives the typical appearance of woody stem without medullary rays. Phloem composed of 3 layers. Xylem tissue wide; xylem vessels were arranged in radial rows separated by rows of longitudinal parenchyma cells and hexagonal vessels; the metaxylem was present towards the cortex and the proto-xylem faced the pith, xylem fibres present. Pith thick, solid and formed of isodiametric parenchyma cells with small intercellular spaces in the middle of the stem.

Fig. 4. *Phlomis aurea* growing in a rocky habitat.

Fig. 5. Opposite decussate leaves of *Phlomis aurea*.

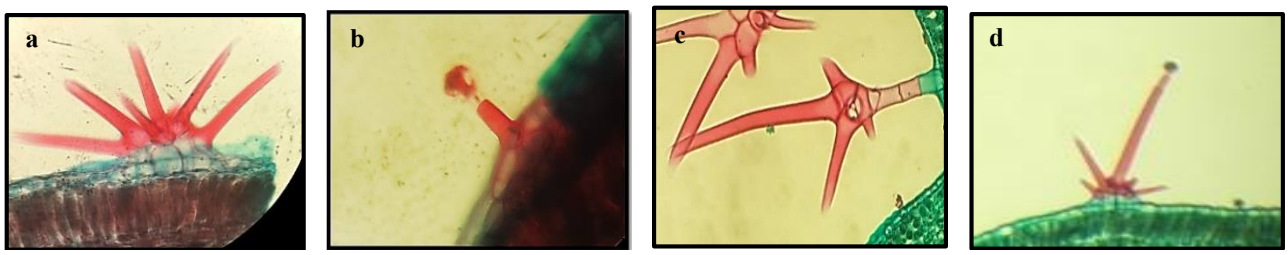

Fig. 6. Indumentum of *Phlomis aurea*
a-stellate trichome, b- type II capitate trichome, c & d- dendroid trichome.

Table 3. Accession numbers and native locality of *Phlomis* species downloaded from GenBank database.

Species	Accession	Native locality	
Phlomis cretica	HQ902764.1	Crete, Jerusalem	Mediterranean species
Phlomis fruticosa	EU627582.1	Albania, Cyprus, Greece, Italy, Turkey, regions of the former Yugoslavia	
Phlomis brevibracteata	KP835739.1	Endemic to Cyprus	
Phlomis crinita subsp. *mauritanica*	AY792671.1	Spain, Morocco, Algeria, Tunisia	
Phlomis lychnitis	AY792634.1	SW Europe	
Phlomis purpurea	AY792672.1	Spain, Portugal, Morocco, Algeria	
Phlomis jeholensis		China	Asian species
Phlomis tuberosa	HM590115.1	China, Kazakhstan, Kyrgyzstan, Mongolia, Russia, SW Asia, Europe	
Phlomis mongolica	HM590103.1	China	
Phlomis umbrosa	HQ839674.1	E Asia, N China, Korea	

Table 4. DNA barcode of *psp*-A/*trn*-H.

	psb-A/*trn*-H	Query coverage %	Similarity %	Genus-level identification status	Species-level identification status
Phlomis jeholensis	FJ513093.1	62	98	✓	×
Phlomis fruticosa	HQ902857.1	57	99	✓	×
Phlomis crinita subsp. *mauritanica*	AY792671.1	58	97	✓	×
Phlomis lychnitis	AY792634.1	58	97	✓	×
Phlomis cretica	HQ902837.1	55	99	✓	×
Phlomis purpurea	AY792672.1	58	96	✓	×
Phlomis lychnitis	AY792630.1	58	96	✓	×

Table 5. DNA barcode of *rbc*L.

	*rbc*L	Query coverage %	Similarity %	Genus-level identification status	Species-level identification status
Phlomis fruticosa	KM360928.1	91	97	✓	×
Phlomis mongolica	HM590103.1	91	97	✓	×
Phlomis jeholensis	HQ839676.1	90	97	✓	×
Phlomis umbrosa	HQ839674.1	90	97	✓	×
Phlomis cretica	HQ902764.1	84	97	✓	×

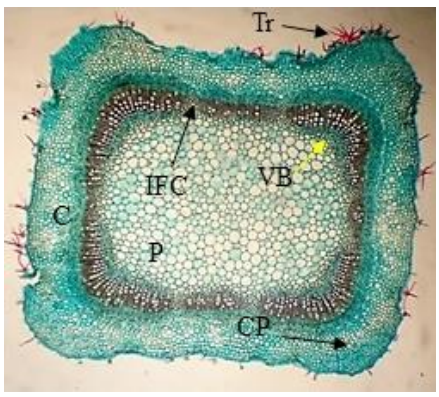

Fig. 7. Transverse section of *Phlomis aurea* stem; Tr = trichomes; VB = vascular bundle; IFC = interfasicular cambium; C = cortex; P = pith; CP = chollenchyma patch

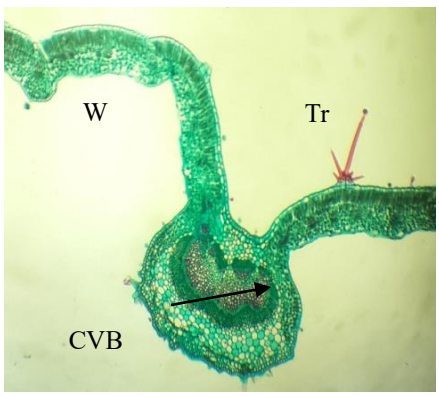

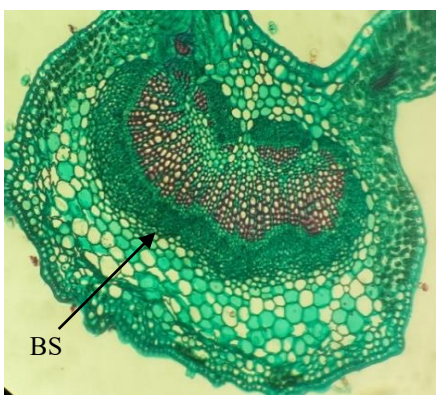

Fig. 8. Transverse section of leaf of *Phlomis aurea*; W = wing; Tr = trichome; CVB = central vascular bundle; BS= bundle sheath

Fig. 9. Transverse section of petiole *of Phlomis aurea*.

Leaf anatomy (Fig. 8 & Table 2)

Leaf consisted of two wings, the midrib zone, and it was dorsi-ventral in a cross section. Cuticle relatively thicker on the adaxial epidermis compared to the cuticle of the abaxial epidermis. Epidermis consists of a single compact layer of mostly radially elongated, barrel-shaped cells (abaxially and adaxially); the adaxial epidermis had smaller sized cells than the abaxial epidermis, diverse types of trichomes were observed on the leaf epidermis-unbranched, non-glandular trichomes, stellate trichomes and dendroid trichomes (see indumentum section and Table 1). Raised stomata were present on the abaxial epidermis, enclosed by kidney-shaped guard cells. Mesophyll tissue composed of one to two layers of palisade cells, with tangentially intercellular spaces and numerous condensed chloroplasts. Smaller size vascular bundles as well as calcium oxalate raphide-type crystals were also detected at the mesophyll tissue. Midrib consisted of central vascular bundles forming a ring surrounded by one to two layers of collenchyma tissue (bundle sheath); two smaller, crescent-shaped vascular bundles were detected at the periphery of the central vascular bundle. These subsidiary bundles constituted the vascular supply for the wings. Phloem well developed and located abaxially. Xylem tissue oriented toward the adaxial side, arranged in radial rows separated by rows of longitudinal parenchyma cells, composed of small, hexagonal xylem vessels. Xylem fibres present; the metaxylem toward the abaxial side, and the protoxylem toward the adaxial side.

Petiole anatomy (Fig. 9 & Table 2)

Petiole circular in a cross section, with two lateral protrusions. Cuticle undulate on both the abaxial and adaxial epidermis. Epidermis comprised of single-layered, oval-shaped parenchyma cells, with capitate glandular and e-glandular trichomes present on both upper and lower epidermis. Cortex consisted of a single layer of collenchyma on the adaxial side; it had 3 layers on the abaxial side and 5-7 layers at the corners. Vascular tissue composed of three unequal, crescent-shaped central vascular bundles, with three subsidiary circular vascular bundles at the corners; the vascular bundles were surrounded by a bundle sheath of collenchyma tissue; the phloem is towards the abaxial.

Phylogeny

Novel sequences of the two cpDNA markers and the *psb*-A/*trn*-H and *rbc*L markers of the endemic *Phlomis aurea* were sequenced successfully. The true sequence length of the *psb*-A/*trn*-H intergenic spacer was 380 bp, the aligned length was 386 bp and the length of the true and aligned sequences of the *rbc*L region was 534 bp. Both sequences were deposited into the GenBank database.

The sequence length of the aligned concatenated dataset was 920 bp, with a region of ambiguous alignment or ambiguous sequences were excluded during the analysis. To obtain a supported phylogeny of the endemic Egyptian *Phlomis aurea*, balanced datasets of *psb*-A/*trn*-

H and *rbc*L were constructed by searching and retrieving all available sequences of *Phlomis* species deposited in the GenBank database (Table 3). Moreover, the two sets were concatenated to enhance the analysis and overcome any deficiencies and inaccuracies that might have resulted from a single marker-based phylogeny. The BI of a concatenated matrix of the two cpDNA sequences produced a total of 202 trees, of which 152 were sampled. The resulting phylogenetic tree comprised of twelve *Phlomis* species as well as *Lamium* sp., and *Eriophyto* sp., as outgroups. *Phlomis* (*s.s*) constitute a monophyletic group (PP = 1). The ingroup is further splits into two clades: the monophyletic Mediterranean clade and non-monophyletic Asian clade. The Mediterranian clade comprises 7 species belonge to the Mediterranian countries. Those species were: *Phlomis lychnitis*: Southern Western Europe, *Phlomis bervibracteata*: endemic to Cyprus, *Phlomis* cretica: Palastain and Crete, *Phlomis fruticose*: Italy, Albania, Cyprus and Turkey, *Phlomis purpurea* and *Phlomis crinite* subsp. *mauritanica*: Portugal, Spain, Morocoo and Algeria and *Phlomis aurea*: endemic to Egypt.Two of those species were endemic. While the Mediterranean clade is will supported (PP=1) it is still unresolved and couldn't be discriminated phylogenetically based on the current sequencing data. On the other hand, the Asian clade composed of five *Phlomis* species native to Asia aminly China. Those species were: *Phlomis mongolica*, *Phlomis tuberosa*, *Phlomis jeholensis*, *Phlomis melanantha* and *Phlomis umbrosa*. The Asian clade was further subdivided into one monophyletic clade and three unresolved sister groups (Fig. 3).

DNA barcoding

DNA barcoding for the endemic *Phlomis aurea* was conducted using the BLAST tool available on the National Centre of Biotechnology Information (NCBI) website. In this study, the newly generated sequences of the cpDNA markers *psb*A-*trn*H and *rbc*L were used as barcodes. Identification on the genus level was successful in both markers. The maximum query coverage percentage of the *psb*-A/*trn*-H and *rbc*L were 62% and 91%, respectively. The maximum similarity percentage was 99% for *psb*-A/*trn*-H and 97% for *rbc*L (Tables 4 and 5). Species-level identification failed when using the same sequences as barcodes.

Discussion

Phlomis aurea grows in diverse types of habitats, including wadi beds, gorges, slopes and basins, at an altitude of 1750–1900 m. It is considered the most frequent endemic species recorded in Saint Katherine protectorate (Zahran *et al.,* 2015). Our results agreed with all the above-mentioned data, except that the recorded altitude for the *Phlomis aurea* collected for the current study was 1600 m. The climatic conditions of the Saint Katherine area are classified as cold desert (Peel *et al.,* 2007). The area is characterized by very hot and dry conditions in the summer, but in the winter, it can be violently cold and dry. Although the gross anatomical features of *Phlomis aurea* are in concordance with the Lamiaceae pattern, the recorded symptoms of adaptation of *Phlomis aurea* to drought stress must be investigated according to the criteria formulated by De Micco & Aronne (2012). Regarding these criteria, the drought stress acclimation strategy of *Phlomis aurea* relies on the presence of thick-walled epidermal cells and a relatively thick cuticle in its vegetative organs, i.e., the stem and leaves. Those structures constituted multi-layered barriers that act as hydraulic controllers that regulate water exchanges between the plant and its surrounding environment. In terms of water translocation under unfavourable conditions such as very low temperatures (freezing) in the Saint Katherine area, the presence of a bundle sheath layer enclosing the vascular cylinder of the stem and leaf has been noted. The xylem elements of *Phlomis aurea* were narrower than other Lamiaceae members. Such specific anatomical features were developed in response to drought stress to improve safety (i.e., the plants were less subjected to cavitation or embolism) though slower water transport (De Micco & Aronne, 2012; Lintunen *et al.,* 2013; Yetişen, 2014). Cavitation is a crucial factor that influences the geographical distribution of plants, and it is useful for figuring out the pattern of distribution of some plant species across habitats (Pockman & Sperry, 2000). This might affect the distribution and isolation of *Phlomis aurea* growing in the Saint Katherine area.

According to Metcalfe & Chalk (1983), the members of Lamiaceae are characterized by a quadrate stem, and patches of sclerenchymatous tissue surrounding the phloem. In the transverse section of *Phlomis aurea*, the stem was quadrangular, and there were small groups of sclerenchyma cells in the outer side of phloem. The quadrangular stem and sclerenchymatous tissue surrounding the phloem groups of vascular bundles have been observed in other members of Lamiaceae. *Phlomis aurea* has raphide crystals in the mesophyll layer of the leaf. Generally, the occurrence and type of crystals are important taxonomical features that have long been used in taxonomy, especially in Lamiaceae members (Metcalfe & Chalk, 1983).

Trichome morphology, structure and distribution in Lamiaceae has been considered to have important taxonomic significance by many authors (El-Banhawy *et al.,* 2016). The sub-familial classification of the family Lamiaceae proposed by Ascensão *et al.,* (1995) was mainly based on the morphology, distribution and frequency of the glandular trichomes. In the current study, *Phlomis aurea* is characterized by three types of trichomes: simple, non-glandular trichomes, three sub-types of capitate trichomes and two sub-types of dendroid trichomes (Table 2). Peltate trichomes have been recorded in *Phlomis russeliana*, which is endemic to Turkey (Cali, 2016). These types of trichomes are not recorded in *Phlomis aurea*. Another unique feature of the endemic *Phlomis aurea* species is the presence of dendroid trichomes, with 10 branches on both the vegetative and floral parts. The dendroid trichome type has been recorded in many genera of the family Lamiaceae. *Phlomis monocephala* is characterized by a dendroid trichome with six branches (Yetişen 2014). *Salvia*

lanigera var. *grandiflora* is characterized by dendroid trichomes with mixed glandular and non-glandular branches (El-Banhawy *et al.,* 2016).

The phylogenetic results showed that Mediterranean clade comprised *Phlomis* species that were distributed in Southern Europe and Northern Africa (Fig 3). The Mediterranean clade represents an unresolved clade corresponding to the unresolved sub-clade from (Bendiksby *et al.,* 2011 and Mathiesen *et al.,* 2011). On the other hand, Asian clade comprises *Phlomis* species that are native to Eastern and Central Asia. Once again, the Asian clade in the current study corresponds to the monophyletic clade I of Mathiesen *et al.,* (2011). The endemic Egyptian *Phlomis aurea* forms an exterior clade within the Mediterranean clade (Fig. 3). Broader sampling within the Mediterranean clade should be included to evaluate its monophyly and proposing infrageneric classification of the whole genus.

The phylogeny of the genus *Phlomis* (*s.l*) was studied by Mathiesen *et al.,* (2011) using *rps*l6 intron and *trn*-L-*trn*-F retrieved a relatively low interspecific resolution within the *Phlomoides*/*Phlomis* lineage. In the current study, an equivalent results have been obtained using DNA sequences of two chloroplast markers *psb*-A/*trn*-H and *rbc*L to reconstruct the phylogeny of the genus *Phlomis* alongside the endemic species *Phlomis aurea*. To resolve the overlap among the Middle Eastern, North African and Southern European lineages, we strongly recommend using other markers such as nuclear genes markers such as (ITS and ETS) to reconstruct the entire whole generic phylogeny. On the other hand, congregating endemic *Phlomis aurea* with Mediterranean clade and grouping the Asian species into one clade do not contradict previous opinions in terms of *Phlomoides*/*Phlomis* (*s.s.*) having a Central Asian geographic ancestral origin, with two centres of distribution from the South to East Asia and Turkey (Mathiesen *et al.,* 2011).

DNA barcoding is currently becoming a reliable method for species identification; a short genetic sequence from a standard part of the genome can be sufficient to verify a plant's identity. The DNA barcode technique is relatively new to the scientific community of Egypt and other low and/or middle-income countries. DNA barcoding was used for the identification of some ornamental and crop plants in Egypt (Elansary *et al.,* 2017). Faried *et al.,* (2018) used DNA barcoding to confirm the identification of *Ephedra* species grown in Egypt. It is highly important to distinguish and recognise the endemic species to help in the conservation of natural resources, especially the medicinally important species such as *Phlomis*. De Groot *et al.,*'s (2011) recommendations for making identifications were applied throughout the current study. On the generic level, DNA barcoding was considered successful when all BLAST searches retrieved percent identity scores of > 95% and involved a single genus. Species identification was considered successful when the percent identity included a single species and scored > 95%. The result of the current study shows success to identify and recognize the genus *Phlomis* using the chloroplast barcodes of *trn*-H-*psb*-A and *rbc*L. According to the results of the current study; we recommend the usage of a combination between chloroplast and nuclear markers as barcodes to identify wild plant in Egypt up to infraspecific level.

References

Akaike, H. 1974. A new look at the statistical model identification. *IEEE. Trans. Automat. Contr*., 19: 716-723.

Bendiksby, M., L. Thorbek, A.C. Scheen, C. Lindqvist and O. Ryding. 2011. An updated phylogeny and classification of Lamiaceae subfamily Lamioideae. *Taxon*, 60: 471-484.

Bentham, G. 1832. *Labiatarum genera et species.* , Ridgeway, London.

Boulos, L. 2002. *Flora of Egypt.* Al Hadara Publishing, Cairo, Egypt.

Cali, I.O. 2016. Anatomy and trichome characteristics of endemic taxon *phlomis russeliana* (sims.) Bentham and their systematic implications. *Bangladesh. J. Bot.,* 45: 297-304.

Chase, M.W., R.S. Cowan, P.M. Hollingsworth, C. Van-den-Berg, S. Madrinan, G. Petersen, O. Seberg, T. Jorgsensen, K.M. Cameron and M. Carine. 2007. A proposal for a standardised protocol to barcode all land plants. *Taxon*, 56: 295-299.

Dereeper, A., S. Audic, J.M. Claverie and G. Blanc. 2010. Blast-explorer helps you building datasets for phylogenetic analysis. *BMC. Evol. Biol.,* 10: 8.

Doyle, J.J. and J.L. Doyle. 1987. A rapid DNA isolation procedure for small quantities of fresh leaf tissue. *Phytochem. Bull.,* 19: 11-15.

El-Banhawy, A., W.M. Kamel and E.M.G. El-din. 2016. *Salvia lanigera* var. *grandiflora* Benth: A new record in the flora of egypt. *J. Ecol. Heal. Env.*, 4: 87-89.

Elansary, H.O., M. Ashfaq, H.M. Ali and K. Yessoufou. 2017. The first initiative of DNA barcoding of ornamental plants from egypt and potential applications in horticulture industry. *PloS one*, 12: e0172170.

Faried, A., A. EL-Banhawy and M. Elqahtani. 2018. Taxonomic, DNA barcoding and phylogenetic reassessment of the Egyptian *Ephedra* L. (Ephedraceae). *Catrina*, 17(1): 1-13

Feinbrun-Dothan, N. 1986. Flora palaestina: Part 4. Text. Alismataceae to Orchidaceae. Jerusalem: *IASH*, 13, 462p.-illus., maps, chrom. nos., keys. En Icones, Maps, Chromosome numbers. Geog 2.

Firdous, S., H. Ahmed, M. Hassuin and M. Shah. 2015. Pollen morphology of *Ajuga* L., *Lamium* L. and *Phlomis* L. (lamiaceae) from district abbottabad pakistan. *Pak. J. Bot*., 47(1): 269-274.

Hall, T.A. 1999. Bioedit: A user-friendly biological sequence alignment editor and analysis program for windows 95/98/nt. *Nucl. Acid Sympos.,* 41: 95-98.

Johansen, D.A. 1940. *Plant microtechnique*. New York Book Company, New York.

Karaca, M., A.G. Ince, A. Aydin and S.T. Ay. 2013. Cross-genera transferable e-microsatellite markers for 12 genera of the Lamiaceae family. *J. Sci. Food Agri.,* 93: 1869-1879.

Khafagi, A., A. O-M, A-E. Sharaf, E. E. Hatab and M. M. Moursy. 2013. Vegetation composition and ecological gradients in Saint Katherine Mountain, South Sinai, Egypt. *JAES*., 13: 402-414.

Kress, W.J., D.L. Erickson, F.A. Jones, N.G. Swenson, R. Perez, O. Sanjur and E. Bermingham. 2009. Plant DNA barcodes and a community phylogeny of a tropical forest dynamics plot in panama. *Proceed. Nat. Acad. of Sci.*, 106: 18621-18626.

Leticia, J. El-Naggar and L. Jack. 1980. Beal. Iridoids. A review. *J. Nat. Prod*., 43(6): pp. 649-707.

Levin, R.A., W.L. Wagner, P.C. Hoch, M. Nepokroeff, J.C. Pires, E.A. Zimmer and K.J. Sytsma. 2003. Family-level relationships of onagraceae based on chloroplast rbcl and ndhf data. *Amer. J. Bot.,* 90: 107-115.

Lintunen, A.,T. Holtta and M. Kulmala. 2013. Anatomical regulation of ice nucleation and cavitation helps trees to survive freezing and drought stress. *Sci. Rep*., 3.

Mathiesen, C., A.C. Scheen and C. Lindqvist. 2011. Phylogeny and biogeography of the lamioid genus *Phlomis* (Lamiaceae). *Kew Bull.*, 66: 83-99.

Metcalfe, C.R. and L. Chalk. 1983. *Anatomy of the dicotyledons*. Oxford.

Nylander J. 2004. *Mrmodeltest*, version 2, Evolutionary Biology Centre. Uppsala University, Uppsala, Sweden.

Oran, S. 2015. Ultrastructure of pollen grains of the genus *Phlomis* L. (Lamiaceae) in jordan. *IJCRBP* 2: 83-87.

Peel, M.C., B.L. Finlayson and T.A. McMahon. 2007. Updated world map of the köppen-geiger climate classification. *Hydrol. Earth Sys. Sci.*, 4: 439-473.

Pockman, W.T. and J.S. Sperry. 2000. Vulnerability to xylem cavitation and the distribution of sonoran desert vegetation. *Amer. J. Bot.*, 87: 1287-1299.

Rambaut, A. and M. Suchard and A. Drummond. 2013. Tracer, version 1.6 computer program.

Ronquist, F., M. Teslenko, P.V.D. Mark, D.L. Ayres, A.H. Darling, S. Ohna, B. Larget, L. Liu, M.A. Suchard. and J.P. Huelsenbeck. 2012. Efficient bayesian phylogenetic inference and model selection across a large model space. *Syst. Biol.*, 61: 539-542.

Sang, T., D.J. Crawford and T.F. Stuessy. 1995. Documentation of reticulate evolution in peonies (*Paeonia*) using internal transcribed spacer sequences of nuclear ribosomal DNA: Implications for biogeography and concerted evolution. *Proceed. Nat. Acad. of Sci.*, 92: 6813-6817.

Stöver, B. and K. Müller. 2010. Treegraph 2: Combining and visualizing evidence from different phylogenetic analyses. *BMC Bioinformatics*, 11: 7.

Swofford, D.L. 2003. Paup*. Phylogenetic analysis using parsimony (* and other methods). Version 4.

Täckholm, V. 1974. *Student's flora of Egypt*. Cairo University, Cairo.

Theodoridis, S., A. Stefanaki, M. Tezcan, C. Aki, S. Kokkini and K.E. Vlachonasios. 2012. DNA barcoding in native plants of the labiatae (Lamiaceae) family from chios island (Greece) and the adjacent cesme-karaburun peninsula (Turkey). *Mol. Ecol. Res.*, 12: 620-633.

Thompson, J.D., D.G. Higgins and T.J. Gibson. 1994. Clustal w: Improving the sensitivity of progressive multiple sequence alignment through sequence weighting, position-specific gap penalties and weight matrix choice. *Nucl. Acids Res.*, 22: 4673-4680.

Yetisen, K. 2014. Morphological and anatomical study of the endemic species *Phlomis monocephala* (Lamiaceae). *Phytol. Balcan.*, 20: 49-55.

Yuzbasioglu, E., M.Y. Dadandi and S. Ozcan. 2008. Natural hybridization between *Phlomis lycia* D. Don x P. *bourgaei Boiss*., (Lamiaceae) revealed by rapd markers. *Genetica*, 133: 13-20.

Zahran, M.A., A.M. Wafaa, A.A. Samy and G.N. Omran. 2015. Endemic species in Sinai peninsula, Egypt, with particular reference to Saint Katherine protectorate: I- ecological features. *J. Environ. Sci.*, 44: 589-609.

(Received for publication 1 March 2018)